International Journal of Chemical and Biochemical Sciences
(ISSN 2226-9614)

Journal Home page: www.iscientific.org/Journal.html

Recent research developments in electrodeposited thin films

Ho Soonmin[1,*], Auttasit Tubtimtae[2], Mahmood Alhaji[3]

[1,*]Faculty of Health and Life Sciences, INTI International University, 71800, Putra Nilai, Negeri Sembilan, Malaysia.
[2]Department of Physics, Faculty of Liberal Arts and Science, Kasetsart University, Kamphaeng Saen Campus, Nakhon Pathom 73140, Thailand
[3]Physics Department & Laser Center, Universiti Teknologi Malaysia, Skudai: 81310, Johor, Malaysia.

Abstract

There are several physical and chemical deposition techniques that were used to produce thin films. The electrodeposition method has many advantages including simple, cheap method and could produce films for large scale production. Many researchers have synthesized binary, ternary, and quaternary films onto various types of substrates (soda lime glass, FTO, silicon, ITO substrate). Thin film based solar cell has been developed using new materials due to low-cost technology, scalability, and manufacturability. Solar energy is renewable energy, the cleanest energy and can reduce greenhouse gases. In this work, photovoltaic performance of different absorber materials (with simple solar cell devices) has been reported. The photovoltaic properties such as fill factor, power conversion efficiency, open circuit voltage, and short circuit current were studied using simulated AM 1.5 sun illumination of nanostructured films. On the other hand, the structure, morphology, and optical properties of the obtained films have been studied by using different tools. Experimental results showed that an annealing process has been used to increase the grain size, control the band gap value, and improve crystallinity of the obtained films.

Keywords: Electrodeposition, thin films, energy efficiency, renewable energy system, photovoltaic, band gap, semiconductor

Full length article *Corresponding Author, e-mail: soonmin.ho@newinti.edu.my

Introduction

In recent years, nanotechnology has attracted great attention [1] due to excellent performance in optics [2], high resistant coating, photonics, magnetic, micro mechanics, and electronics [3]. Nano materials could be categorized into zero dimensional (quantum dots in photovoltaic cells) [4], one dimensional (nanotubes, nanorods and nanowires) [5] and two dimensional (thin films in optical coatings). Synthesis of nanostructured thin films onto substrate has been reported by many researchers [6-9]. Several deposition methods such as physical and chemical deposition techniques [10,11] have been chosen for the formation of binary, ternary, and quaternary films. Generally, operational cost, properties of the desired films and application of the final product affected the choice of deposition method [12,13]. In the pulsed laser deposition method, a high energy pulsed laser was employed to irradiate target material, then its vapor will be deposited onto a substrate [14]. It was noted that samples (such as ceramics, metals, semiconductor materials) with varied thickness could be observed using this method [15]. It can be concluded that this technique is suitable for depositing materials that are not easily evaporated using thermal methods [16], such as high-melting-point materials and materials that are prone to oxidation. Synthesis of semiconductor thin films (crystal and non-crystalline materials) onto different types of substrates [17]. Electrodeposition method is processed by the action of an electric current passing in an electrochemical plate, two conductive or semi-conducting materials immersed in an electrolyte as electrodes. Film thickness is chiefly dependent on the deposition time. Generally, thicker films could be deposited at longer time, and vice versa. Electrodeposition technique is one of the non-vacuum methods [19] to produce semiconductor materials [20]. Most of the prepared materials undergo annealing process to achieve uniform morphology [22, 23]. Phase change (liquid to solid) could be observed via electro deposition method if compared to molecular beam epitaxy and metal oxide chemical vapor deposition, which directly changes from gas to solid phase. Eventually, high quality materials could be formed. In addition, the available source of electrons (cathode surface) should provide better growth conditions, fulfilling the charge neutrality Advantages of electrodeposition included low-cost method, low energy consumption, environmental technique, lower material waste, and could produce thin films using low temperature. Film formation process, and fundamental properties could be controlled using applied potential. The biggest issue was that it was unsuitable for large-scale

production. This deposition process should be improved to achieve ideal conditions. So that, the obtained films could be employed in a wide range of applications [18]. In this work, electro deposition method has been used to prepare various types of films (binary, ternary, quaternary and penternary) onto substrate. The properties of the obtained films have been investigated using XRD, FESEM, XPS, Raman spectroscopy, EDX, AFM and TEM. Lastly, the photovoltaic properties (open circuit voltage, fill factor, power conversion efficiency, and short circuit current) were investigated using simulated AM 1.5 sun illumination of nanostructured films.

1. Binary thin films

Zinc oxide films have been grown onto ITO substrate [26], using zinc chloride (as source of Zn^{2+} ions) and platinum foil (counter electrode). Experimental results confirmed that the most stable form was wurtzite phase (crystallite size=10.2 nm), however flower-like shapes also could be observed because of lack of equilibrium conditions. XRD data displayed the major peak at 36.26□, attributed to (101) plane. TEM images (figure 1) highlighted transition of amorphous layer ($Zn(OH)_2$) to ZnO via nucleation and growth process. The band gap was 3.13 eV, could absorb visible light effectively. Indium tin oxide (ITO) coated glass substrate [27] has been used to prepare zinc telluride films (pH=4, precursors=zinc sulphate and TeO_2, temperature=313K,anode electrode=pure Au wire, reference electrode=Ag/AgCl). Stochiometric films with thickness of 3μm could be observed when the deposition potential was -0.8V. The as-deposited films showed black tint (figure 2), amorphous phase, and resistivity of $2x10^5$ □m. While, annealed films (at683 K, 5 hours) indicated reddish-brown tint, crystallinephase, band gap value of 2.3 eV and resistivity value of $2x10^3\Omega m$. Cerium oxide films have been employed as buffer layer (superconductor material), anticorrosion coating (metals) and structure barrier (insulator on silicon). Nanostructured CeO_2 (111) oriented films have [28] been deposited onto stainless steel substrate, at pH 7.5, using sodium acetate (ligand) and cerium nitrate. Raman analysis showed homogeneities of films, a peak at 450 cm^{-1} corresponding to CeO_2. In the XRD investigations, polycrystalline films could be prepared using galvanostatic deposition mode, current density lower than -0.06 mA/cm^2 and temperature more than 50 □C. Based on the SEM images, un-sintered films displayed smooth surface with cracking because of mismatch between films and substrate. In addition, cracking of films could be observed during the sintering process or using other deposition methods such as wet chemical techniques. Tungsten trioxide is n-type semiconductor, can be used in lithium-ion battery electrodes, reversible electrochromic elements, gas sensor and smart windows. The ITO glass was rinsed with acetone and water to removecontaminants. The ITO substrate [29] and platinum plate arefixed in the holder, so that the electrode distance was 20 mm. During the formation of films, electrodeposition current and electro deposition time were varied. Experimental findings confirmed that surface roughness and thickness increase when the electrodeposition time and electrodeposition current was increased. In the XRD analysis, amorphous phase couldbe observed in the as-deposited films and annealed films (250 ˚C), however, triclinic phase could be seen at higher temperature (500 °C and 700 °C). SnO_2 could be employed in lithium-ion batteries, gas sensor and solar cell applications. However, lower efficiency is due to several reasons such as low conduction band edge and severe charge recombination. Nano porous films have been deposited on titanium substrate [30], in the electrolytic bath (0.05 M of $SnCl_2$ and 0.1 M nitric acid) at 75 C. Dye-sensitized solar cells (DSSC) is consisted of SnO_2 films, covered with molecular dye (N3) that adsorb sunlight. The electrolyte of solar cell contains 0.1 M of iodine, 0.6 M of dimethylpropylimidazolium iodide, 0.1 M of lithium iodide and 0.5 M of 4-tertbutylpyridine. As shown in Table 1, addition of nitric acid improved fill factor and short circuit current due to an increase of surface roughness. Power conversion efficiency reached 0.35% after UV-treatment because of the improvement of crystallinity. Cuprous oxide is a p-type semiconductor, member of I-VI groups and was used in solar cell applications (abundant, suitable band gap, could be produced via cheap deposition method). Generally, electro deposition of cuprous oxide undergoes two steps, reduction of copper (II) ions to copper (I) ions and precipitation of copper (I) ion to Cu_2O films [equation 1 and 2]. El-Shaer and Abdelwahed [31] have demonstrated the electro deposition of nanostructured films on fluorine doped tin oxide (FTO) substrate using cupric acetate, at deposition potential of -0.5 V versus Ag/AgCl. Good quality films (crystalline with cubic phase) with some spherical grains could be synthesized in 10 minutes.

Indium sulfide films were semiconductors, member of III-VI group, were used in solar cell applications (as buffer layer) due to wide band gap, stability, non-toxic materials, and excellent photoconductive properties. According to EDX studies, nearly stoichiometric ratios [32] could be seen (molybdenum coated glass as substrate) in the organic bath (ethylene glycol). Ag/Ag/Cl and graphite were used as reference electrode and counter electrode, respectively in three electrode chemical cells. The optimized experimental conditions were reported based on the Taguchi Method (temperature=160 °C, deposition potential= -0.6 V Ag/AgCl, time=180 seconds, composition of solution=0.1M Sulphur +0.1M $Na_2S_2O_3$+0.1M NaCl+0.05M $InCl_3$). Researchers have observed that deposition temperature showed the least impact and deposition potential indicated the biggest impact upon the stoichiometric. Fabrication of copper telluride films onto indium doped tin oxide (ITO) glass slides using three-electrode cell [33]. XRD, SEM, EDX and UV-visible spectrophotometer studies of the CuTe (orthorhombic phase with crystal size of 92.11 nm, bigger size with more distinct morphology, band gap=1.5 eV, atomic percentage of Cu:Te is 50.4:49.6) and Cu_2Te films (hexagonal phase with crystal size of 36.84 nm, smaller size with more compact morphology, band gap=1.12eV, atomic percentage of Cu:Te is 67.3:32.7) have been conducted and reported. Molybdenum disulfide film showed excellent lubrication properties due to its layered structure. It could be used in hydrodesulfurization of petroleum (as catalyst), solarcell applications (band gap of 1.7 eV), photochemical production of hydrogen. Several deposition techniques such as chemical vapor deposition, wet inorganic solvent route andtemplate-based process have been used to maximize sulfide edge effect on hydrogen production. Nanostructured MoS2 films were grown onto different types of substrates [34] fromelectrolytic bath (sulfide and molybdate ions). There are threefeatures that were described according to

UV-visible spectrum in the annealed films (500 □C, 5 hours). It was noticed that two excitons (B =625 nm, C=682 nm) attributed to interlayer interactions, while A exciton corresponds to Mo-S bond. Based on the FTIR spectra, peaks at 472 cm^{-1} and 690cm^{-1} were contributed to Mo-S vibration of MoS_2, and (Mo- O) vibration, indicating co-existence of oxide and sulfide in the obtained samples. In terms of phase and crystal structure studies, amorphous phase could be seen in as-deposited films(NiP substrate). It was noted that intensity of hexagonal (002) plane increases when the annealing temperature (heating rate was 5 □C/min) was increased. Surface morphology investigation has been conducted using FESEM technique for the films prepared using different substrates such as NiP (nanorod and nanotubes), CoW (hollow dumb-bell shape) and copper substrate (cracks and film delamination). TEM images of annealed films (600 □C, 120 minutes) showed nano ball (size=5 nm to 10 nm), nanoribbons (width=10nm) and length (few nanometer). Researchers have summarized that production of nanosheets from amorphous phase, then, formed nanorod, nanotube and other structures. multiple the obtained samples were multiple in layers, and production of hexagon.

2. Ternary thin films

The as-deposited $CuInTe_2$ films are amorphous and adhered well to the titanium substrate [35]. In terms of morphology studies, the obtained films show grain morphology and uniform structure. Ishizaki and co-workers [36] have reported that flat and smooth films were prepared at 303 K (substrate-titanium, pH=1, deposition potential=- 660 mV versus Ag/AgCl, precursors= $5x10^{-4}$ M TeO_2, $2.5x10^{-4}$ M $CuCl_2$, 1x10-2 M $InCl_3$), while polycrystalline films with closely stoichiometric composition were depositedat 363 K. Based on the cathodic polarization curves, electro deposition of copper (-200 mV versus Ag/AgCl), indium (- 600 mV), tellurium (-120 mV) from an acidic bath could be observed clearly. Formation of $CuInTe_2$ films have been highlighted (equation 1 to 3). EDX studies [37] confirmed that deposition potential affected the atomic percentage of copper, indium, and tellurium (Table 2) in the as-deposited films (complexing agent=citric acid, pH=2, temperature=80 ˚C, substrate=FTO, counter electrode=graphite sheet, reference electrode=Ag/AgCl) and annealed samples (400C, 15-20 minutes). Obviously, all the films showed tellurium rich composition. In addition, ratio of copper/indium was found to be more than 1 (higher deposition potential) in annealed films. Solar cells were fabricated (ITO/CdS/CIT/Au), tested using solar simulator (1.5 AM, power intensity=100 $mWcm^{-2}$), and the cell parameters were reported (fill factor=43 %, efficiency=4.13 %, short circuit current density=20 mA/cm^2, and open circuit voltage=480 mV). Mahalingam and co-workers [38] have demonstrated the preparation of films using three electrode systems (substrate=ITO glass, precursors=$CuSO_4$, TeO_2, $In_2(SO_4)_3$, reference electrode=saturated calomel electrode). Film thickness was measured using stylus profilometer. Irregular growth with rough surface was found at lower temperature (less than 50 °C), while film formation was hindered at higher temperature (more than 65 °C) because of hydrogen evolution process. However, thicker films could be observed because of an increase in the solubility of TeO_2 when the deposition temperature was increased. It was noted that a very low concentration of tellurium is required during the formation of films. Because of tellurium was less electropositive if compared to copper and indium. Based on the experimental results, free tellurium is deposited successfully onto substrate at pH 3, however, precipitation of TeO_2 was observed when the pH was 4.

$$Te + 2H^+ + 2e^- = H_2Te \ [E\ 1]$$
$$2Cu^{2+} + HTeO^+ + 3H^+ + 8e^- = Cu_2Te + 2H_2O \ [E\ 2]$$
$$2In^{3+} + 3H_2Te = In_2Te_3 + 6H^+ \ [E\ 3]$$
$$Cu_2Te + 3H_2Te + 2In^{3+} = 2CuInTe_2 + 6H^+ [E\ 4]$$

The p-type copper antimony selenide ($CuSbSe_2$) is a chalcogenide semiconductor, could be used in thermos electric, infrared detectors, and optoelectronic applications. Also, this semiconductor has been applied as absorber material for solar cell applications due to high absorption coefficient (lone pair electron in orbital $5s^2$ present in trivalent antimony). In addition, a 2-dimensional structure was observed, produced chemically inert surfaces, reduced the losses of carrier recombination. So far, the power conversion efficiency was very low, strongly depending on the deposition method such as reactive close-spaced sublimation process (efficiency=3.04% [39]), low-temperature pulsed electron deposition (efficiency=3.8% [40], high throughput experimental and hydrazine solution process (efficiency=2.7% [41]). Polycrystalline with orthorhombic phase [42] of films have been produced at the deposition potential of -0.4V versus SCE. The annealed films indicated a band gap of 1.1 eV, excellent absorption coefficient value ($7x10^4$ cm^{-1}) and carrier concentration of 5.8 x 10^{17} cm^{-3}. Nanostructured films have been grown onto FTO substrates using three-electrode cell system [43] at room temperature (precursors=copper chloride, selenious acid, antimony potassium tartrate, supporting electrolyte=ammonium chloride, pH=2, deposition potential=-0.4 V saturated calomel electrode, deposition time=30 minutes). Based on the linear sweep voltammetry analysis (figure 3), we can observethat the electrodeposited samples were very sensitive to potential variation. The best deposition potential was -0.4V versus SCE to produce nearly stoichiometric composition. In the morphological studies, as-deposited films showed spherical grains (250 nm), homogeneous, compact, copper and selenium poor composition.

Table 1: Photovoltaic parameters based on the SnO_2 films under various types of treatment.

Post treatment conditions	Short circuit current	Open circuit voltage	Efficiency(%)	Fill factor
Pure water vapor treatment	0.6 mA/cm^2	329 mV	0.09	0.48
Nitric acid (HNO_3) treatment	1.11 mA/cm^2	329 mV	0.23	0.62
Ultra- violet treatment	1.65 mA/cm^2	340 mV	0.35	0.63
Calcined at 550 □C	4.22 mA/cm^2	334 mV	0.52	0.37

Table 2: Elemental composition of as-deposited films and annealed films deposited under different deposition potentials [37].

Deposition potential	Atomic percentage (%)					
	As-deposited films			Annealed films		
	Cu	In	Te	Cu	In	Te
-0.75	23.14	20.8	56.06	20.34	19.76	59.9
-0.7	22	18.26	59.74	21.07	19.17	59.76
-0.65	21.04	14.9	64.06	18.75	20.84	60.41
-0.6	15.14	26.02	58.84	15.46	26.21	58.33

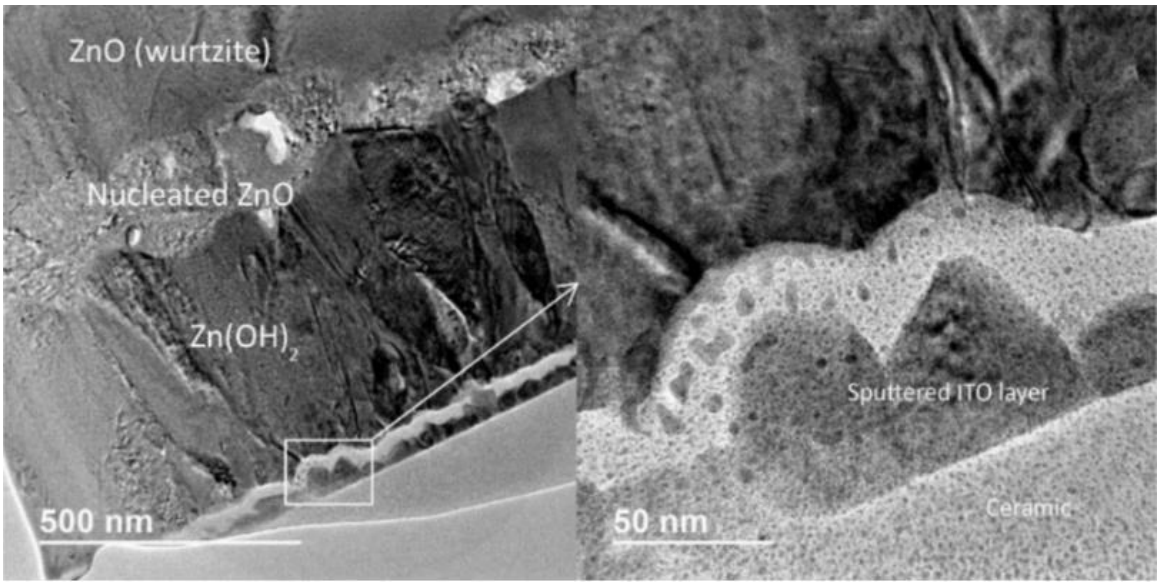

Figure 1: TEM image of electrodeposited ZnO wurtzitephase [26].

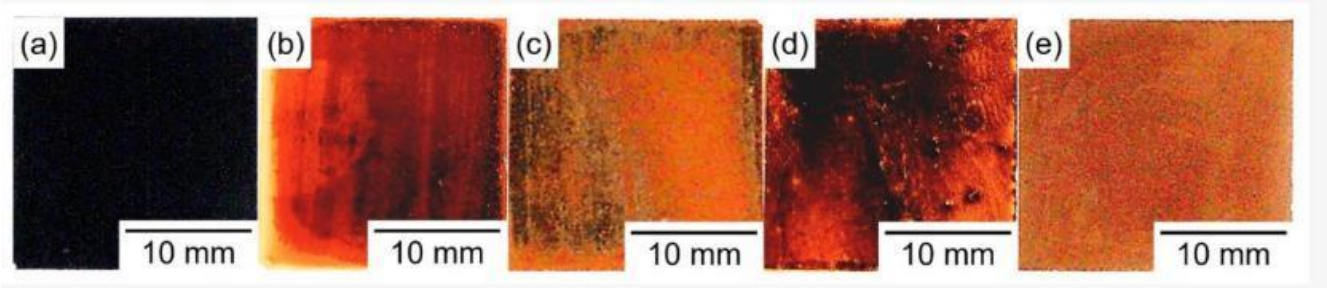

Figure 2: ZnTe films prepared under different annealing temperatures (a) as-deposited films (b) 653 K (c) 663 K (d) 673 K (e) 683 K [27]

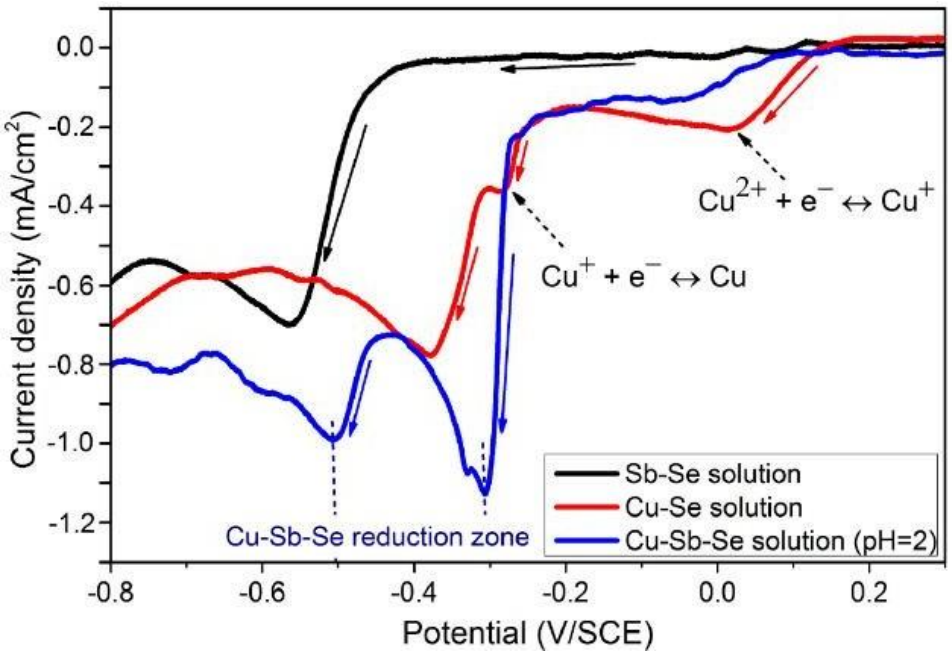

Figure 3. Voltammograms thin films deposited onto FTO- coated substrate in Cu–Se, Sb–Se and Cu–Sb–Se solutions [43]

Table 3: Raman spectroscopy modes for electrodeposited$CuSbSe_2$ annealed at different temperatures [43]

Temperature (°C)	Raman shift(cm^{-1})	Phase
250 and 300	89 105 144 154 217 264 189	$CuSbSe_2$ $CuSbSe_2$ $CuSbSe_2$ $CuSbSe_2$ $CuSbSe_2$ $Cu_2SeSb_2Se_3$
350	208 217 167	$CuSbSe_2$ $CuSbSe_2$ Cu_3SbSe_3
400	187 169 230 83 106 144 217 259	Cu_3SbSe_3, $Cu_3SbSe_4Cu_3SbSe_4$ $Cu_3SbSe_4CuSbSe_2$ $CuSbSe_2$ $CuSbSe_2$ $CuSbSe_2$ Sb_2O_3
450	259 89 194 258 376	Cu_2Se Sb_2O_3 Sb_2O_3 $Sb_2O_3Sb_2O_3$
500	107 144 217	$CuSbSe_2$ $CuSbSe_2$ $CuSbSe_2$

Table 4: Photovoltaic properties of the $AgCuO_2$ films [44]

Depositiontime (s)	Fill factor	Open circuit voltage	Short circuit current	Efficiency
30	58.8 %	1.06 V	16.44 mA/cm^2	10.24 %
45	54.7 %	0.96 V	14.04 mA/cm^2	7.37 %
60	49.9 %	0.79 V	11.26 mA/cm^2	4.43 %

Table 5: Comparison of XPS data in the obtained as- deposited films and annealed samples [48].

Element	As-deposited films		Excessively annealed films (above 350 □C)	
	Height	Area	Height	Area
Copper +oxide	14479 counts	111 kc eV/s	9576 counts	47 kc eV/s
Indium +oxide	4336 counts	31 kc eV/s	24073 counts	186 kc eV/s
Selenium +oxide	5284 counts	26 kc eV/s	3394 counts	48 kc eV/s

Table 6: Structural and compositional of the as-deposited films and annealed films [50]

				Lattice constants (Å)			Atomic(%) ratio		
Temperature (°C)	Bragg angle (°)	FWHM (°)	Grain size (nm)	a	c	Strain ($x10^{-2}$)	Cu	In	Se
As-deposited	26.88	1.05	8	5.73	11.511	1.9			
250	26.68	0.17	46	5.751	11.595	0.304	21.92	13.81	64.26
300	26.74	0.14	58	5.77	11.474	0.25	29.41	17.47	53.11
350	26.45	0.12	67.3	5.775	11.5	0.206	26.14	22.83	51.03
400	26.44	0.11	73.4	5.776	11.505	0.203	8.42	23.33	48.25

Table 7: Compositional and thickness of the samplesdeposited under different conditions [53].

Concentration of $SnSO_4$	Deposition potential (V versusSCE)	Thickness	Cu:Sn:S:O ratio
3 mM	-0.80	0.5 µm	1.7:0.084:0.13:1
6 mM	-0.82	0.3 µm	2.1:0.5:0.6:1
9 mM	-0.85	0.35 µm	2.1:0.49:0.79:1
12 mM	-0.87	0.3 µm	2.6:0.71:0.9:1

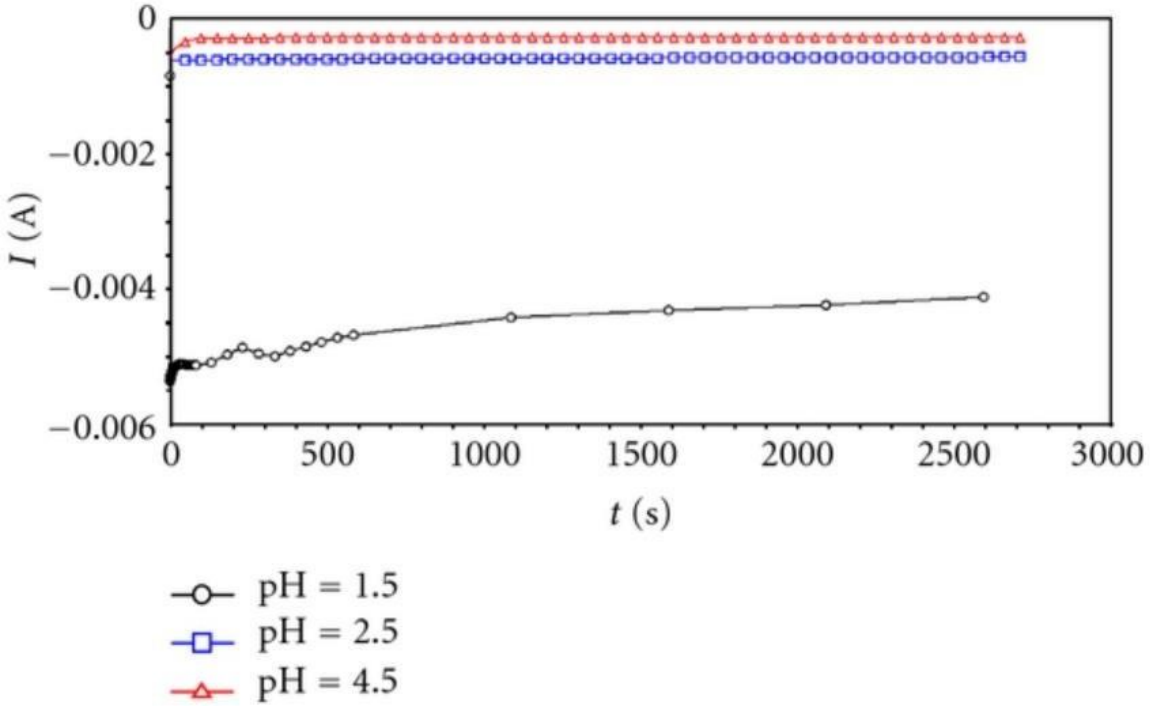

Figure 4: Chronoamperometry curves of electrodeposited Cu-In-S films at different pH values [51]

Table: 8: Properties of the films deposited under different atmospheres [59]

Atmosphere	Band gap (eV)	Morpholog y study (FESEM)	Compositi on study (EDX)	Structura l study (XRD)
Argon	1.48	Compact, bigger flatgrain	sulfur poorcomposition	Few peaks at(112), (200), (220), and (312) directions.
Nitrogen	1.76	Well- defined grains with average grain sizesmaller than 0.5 μm	Sulfur poorcomposition	The intensity of (112) peak decrease s
Nitrogenand hydrogen sulfide	1.53	densely packed, compact morphology, grain size was1 μm	sulfur richcomposition	The sharpest diffraction peaks could beseen.

Table 9: Properties of the prepared films using different methods [63].

	DC electrodepositionmethod	DC electrodeposition plus mechanical perturbations
Color of thefilms	Dark gray	Silvery gray
Compositional	Cu (23.41%), In (17.76%), Ga (8.05%), Se (50.78%)	Cu (22%), In (16.79%), Ga (6.82%), Se (54.39%).
Power conversion efficiency (%)	0.56	2.79
Fill factor	0.25	0.322
Open circuitvoltage (mV)	308	306
Short circuit current (mA/cm^2)	7.35	28.38
Band gap (eV)	1.12	1.16
Thickness (μm)	1.2	0.9
Crystallite size(nm)	26.6	26.7
Diffractionpeak	2θ=26.62°, 27.62°, 35.56°, 44.18°, and 52.38°	2θ=26.84°, 27.92°, 35.78°, 44.56°, and 52.78°
Morphologystudy	Isolated nodules,cauliflower-like	More compact

Table 10: Properties of the films using selenium dioxide andpure selenium

	Pure selenium	Selenium dioxide
Gran size (nm)	65.92	57.72
FWHM	0.2785	0.2671
Short circuit current(mA/cm^2)	0.143	0.376
Open circuit voltage(V)	1.449	2.037
Efficiency (%)	0.079	0.403
Fill factor (%)	0.384	0.526
Band gap (eV)	1.03	1.06
Atomic percentage		
Copper (%)	16.86	6.37
Indium (%)	18.47	18.13
Selenium (%)	0.67	14.36
Gallium (%)	1.33	2.14
Ratio of Ga/(Ga+In)	0.067	0.106

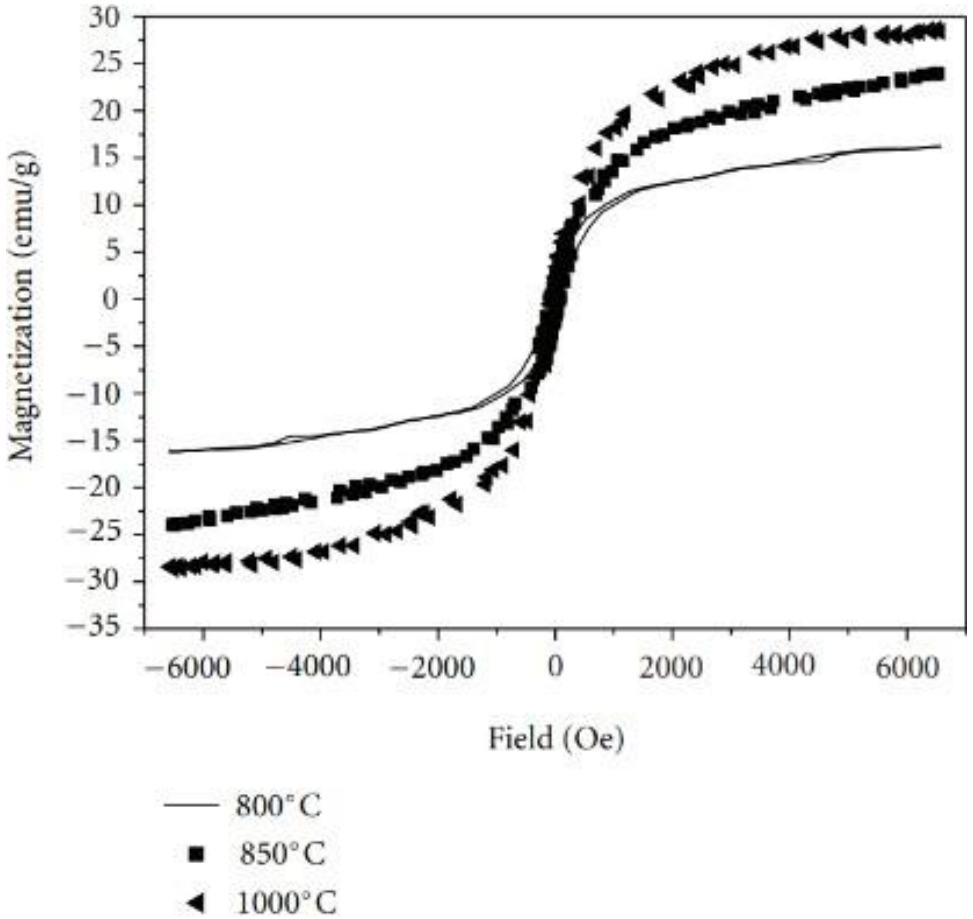

Figure 5: The influence of annealing temperature on the magnetic hysteresis loops of $Ni_{0.5}Zn_{0.5}Fe_2O_4$ films [54].

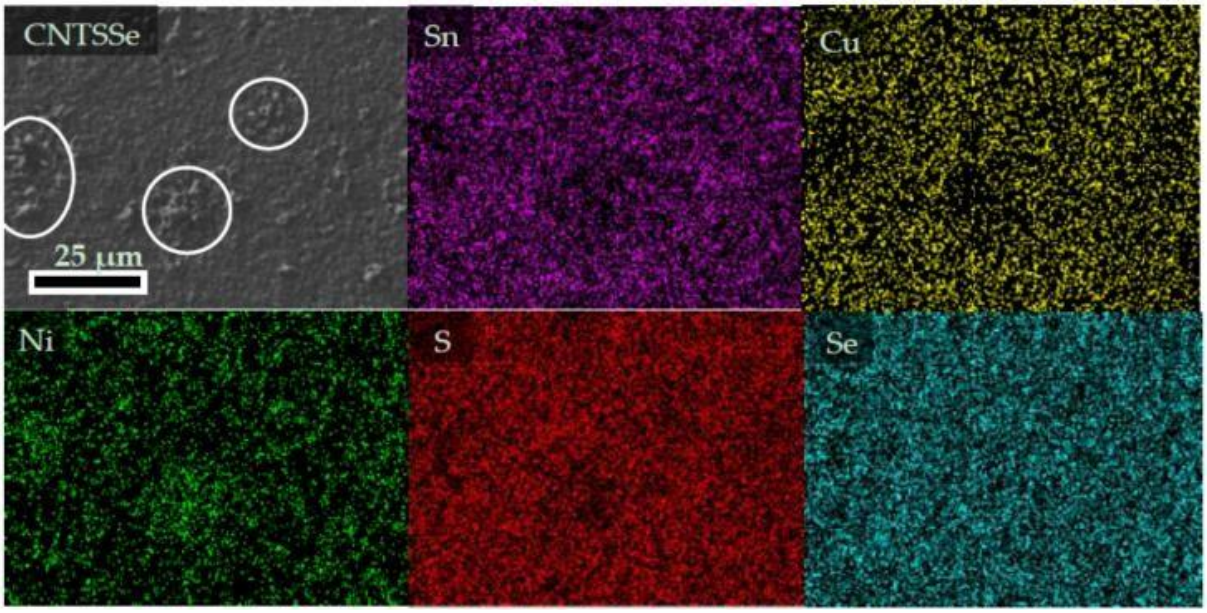

Figure 6. SEM image (top view) and EDX mapping imagesof the CNTSSe thin films [69]

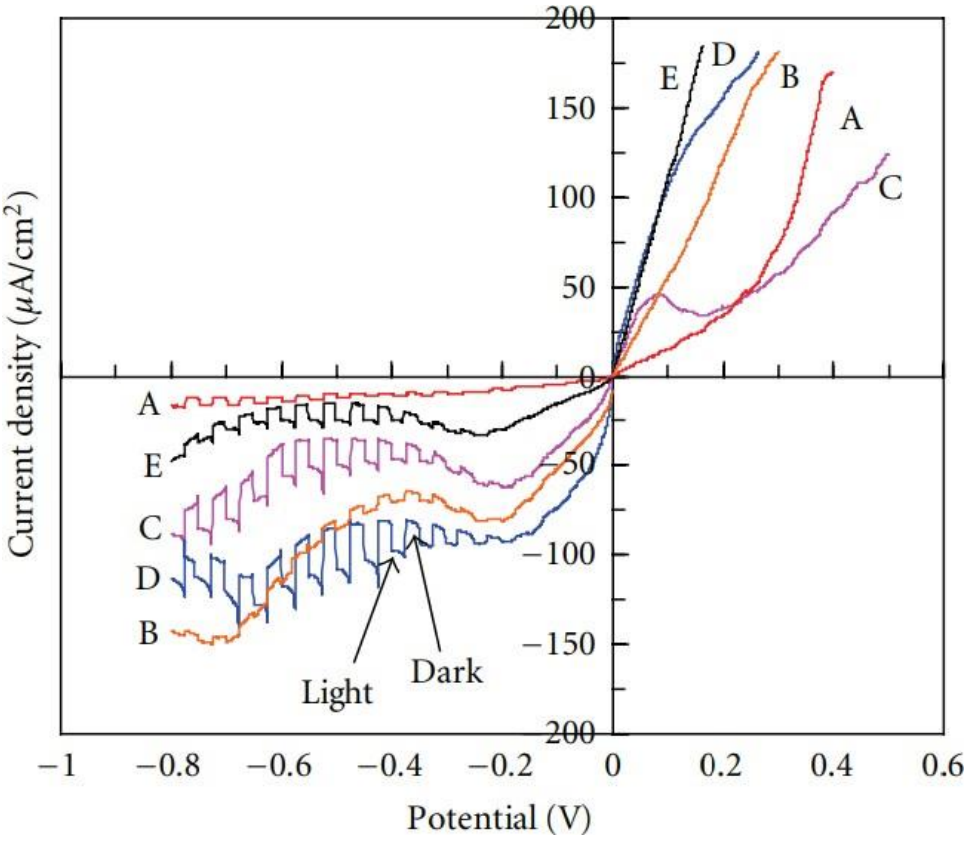

Figure 7: PEC analysis of the CZTSO films [70].

Table 11: Properties of electrodeposited CZTSO films [70]

	Sample				
	A	B	C	D	E
Potential (V)	-0.8	-0.8 to-0.5	-0.9to-0.5	-1to-0.5	-1.1to-0.5
Zn (%)	9.4	11.3	8.4	16.3	17.4
Sn(%)	12.9	8.8	14.8	13	13.2
S(%)	19.8	30.9	40.9	28.8	26
O (%)	29.7	20.6	8.4	19.2	19.6
Cu(%)	28.2	28.4	27.6	22.6	23.6
Thickness (□m)	0.5	0.3	0.3	0.3	0.3
Band gap(eV)	2.1	1.6	1.6	1.5	1.6
XRD peak	(112), (200) and (303)	(112), (200) and (312)	(112), (200) and (312)	(112), (200) and (312)	(112), (200) and (312)

However, significant changes in the morphology and composition (Table 3) couldbe found when the films were heated at 250 °C (grain size of 125 nm, rougher surface), 300 °C (grain size of 400 nm, uniformly surface), 350 °C (more compact, grain size of 250nm), 400 °C (porous structure), 450 °C (layer shrinks, larger agglomerates) and 500 °C (unclear boundary, rail-like appearance). According to the EDX studies, silicon and tin content were increased (450 °C and 500 °C) due to thethinning and shrinkage of the films. The Cu/Sb ratio was increased to 3.86 (400 to 500 °C) because of Sb_2Se_3 sublimation process. The Sb/Se ratio was smaller than 0.14 due to formation of Cu_2Se. Oxygen comes from the formation of Sb_2O_3 (270 °C to 360 °C). Further investigate the phase formation using Raman spectroscopy was reported also (Table 3). The p-type $AgCuO_2$ films were used as the hole transport layer in the perovskite solar cells because of chemical stability and low-cost. Inorganic materials (WoO, NiO, MoO, CuO, and CuSCN) could be used to replace organic hole transport materials. Several disadvantages of organic hole transport materials (poly(3,4-ethylenedioxythiophene), poly[bis(4-phenyl)(2,4,6-trimethylphenyl) amine], and 2,2′,7,7′-tetra[N,N-bis(4-methoxyphenyl) amino]-9,9′-spirobifluorene) such as non-ecofriendly materials, expensive, very complex synthetic route, and issue of long-term stability. The prepared films in specific conditions (substrate=FTO, reference electrode=Ag/AgCl, temperature=40 □C, counter electrode=platinum plate) showed smooth morphology, free pinhole structure, excellent conductivity, and high transmittance value [44]. It was noted that significant changes could be observed in the morphology and film coverage when the deposition time was 15s (small part of island shaped, very thin layer), 30s (completely covered the substrate, film thickness=80-100 nm), 45s (compact morphology) and 60s (solid sheet array structure, film thickness=150-200 nm) based on the SEM analysis. In the XPS investigations, it is evidence of the fact that the main elements were silver (Ag3d5/2=366.6 eV & 367.8 eV contribute to monovalent & All the $CuInSe_2$ thin films deposited onto ITO glass showed polycrystalline with prominent peaks along (112), (204/220) and (312/116) planes. They also noticed that (112) peak and (204/220) peak increased when the pH was pH 2.6 and pH 2.2, respectively. Kaupmees and co-workers have described the synthesis of thin films using ITO glass from electrolytic bath containing SeO_2, $CuSO_4$ and $In_2(SO_4)_3$ solution. A well adhesivity, homogeneous morphology and smooth layers could be seen when the deposition potential has been changed from higher to lower value (-0.6 V to -1 V versus Ag/AgCl. Shen and co-workers have concluded that smooth, polycrystalline films with different thicknesses (1 □m to 1.6 □m) could be used in tandem solar cells. EDX spectrum showed the atomic ratio of copper, indium and selenium was 1:1.14:2.45, respectively in annealed films (vacuum tubular furnace). Titanium was cleaned with acetone, rinsed with water before could be usedas substrate [48]. In the XPS studies, three regions (Cu2p, Se3d and In3d) could be seen in the obtained as-deposited films(Table 5) and annealed samples (350 □C and 30 minutes, in air). Obviously, the copper content was reduced due to the decomposition of the materials. Direct electrodeposition [49] has been applied for the fabrication of thin films (reference electrode=SCE, deposition potential=-500 mV to -600 mV, substrate=molybdenum coated glass). Nanostructured films with different crystallite size and thickness could be produced for many electronic applications. Bigger crystallite size (32-82 nm) with thin layer (0.799-1.014 μm) could be formed when the temperature was 25 °C and deposition potential of -500 mV versus SCE. In contrast, smaller crystallite size (25-47 nm) with thicker films (1.829-1.979 μm) was obtained at 40 °C and potential of -600 mV. Nanostructured films were grown onto silicon substrate [50] via galvanostatic mode in two electrode cells (deposition time=10 minutes, constant current density=10 mA/cm^2). Structural and composition of the obtained films have been reported (Table 6). The smallest grain size (8 nm) in as-deposited films showed amorphous phase. As shown in table, the number of diffraction peak contribute to chalcopyrite phase increased, but full width ay half maximum (FWHM) of (112) plane reduced, when the annealing temperature was increased. It was noticed that micro-strain decreases at higher annealing temperature because of reduced grain boundaries and increased grain size. The compositional analysis confirmed that the best stoichiometric films was obtained (350 °C) with no loss in selenium content. Based on the optical studies, band gap (1.01 eV), refractive index (2.03) and extinction coefficient (2x10-4) were reported as well. CuInS2 films semiconductor did not contain toxic substances if compared to $CuInSe_2$ and were used for the solar cell application. Dodecylbenzene sulphonic acid [51] has been used to adjust the pH value and as suspending agent during the formation of films (substrate=FTO glass, precursors=copper chloride, indium chloride, sodium thiosulphate, reference electrode=SCE). Solar cells have been made using FTO/$_{CuInS2}$/ZnO/FTO heterojunction devices and showed very low power conversion efficiency (efficiency=1.3x10-2%) and fill factor. Because of high series resistance and surface recombination of electrons at the back contact. According to chronoamperometry studies (figure 4), electrodeposition cathodic current increases when the pH is reduced. When the pH was 1, it was noticed that sharp initial current maximum could be observed, then current plateau region was happened, finally slightly increased with time. Deposition of p-type $CuInS_2$ films was carried out at room temperature [52] (working electrode=ITO glass, counter electrode=platinum plate, reference electrode=saturated calomel electrode, pH=6, complexing agent=citric acid, electrolytic bath=copper chloride, indium chloride and sodium thiosulphate, supporting electrolyte=potassium chloride). Citric acid could be complex with Cu^{2+} ions & In^{3+} ions, moreover, can narrow the redox potentials of In3+/In & Cu^{2+}/Cu, and prevent the formation of metal hydroxide as well. The influence of deposition potential was studied. Results revealed that current increases when the deposition potential was increased. Also, researchers have concluded that current decreases within initial 120 seconds at any potential because of concentration gradients could be seen in the boundary layer very close to the electrode surface. After the initial period, currents at potentials at -0.7 V to -0.9 V are very stable (deposition area increases and rougher surface could be seen), but current increases gradually when the deposition potential at -1 V and -1.2 V (upper layer was removed). On the other hand, XRD pattern and Raman spectroscopy confirmed that the best annealing temperature was 550 °C. Also, Raman analysis showed that all the films contained Cu2-xS phase (except temperature was 550 °C).

Precursor solution is considered as an important factor in determining the properties of films. SEM images indicated that films produced at Cu2+/In3+ ratio was 1:4 showed bigger crystals, condensed films, reduced grain boundaries and cracks. These materials could be used as effective absorber layer due to the largest photocurrent could be observed. Carbon contamination was another issue to produce films using solution -based process. EDX analysis indicated the presence of carbon (3.5 %) in the obtained samples, came from citrated.

3. Quaternary thin films

The p-type CuSnSO films have been grown on ITO substrate [53] using CuSO4, Na2S2O3 and SnSO4. In acidic medium, thiosulphate ions will release sulfur atom. Table 7 shows thickness and composition for the films deposited under different concentration of SnSO4 solutions. Obviously, tin and sulfur content increase with increasing the concentration of SnSO4. In addition, larger oxygen content (dissolved oxygen in the solution) could be observed if compared to sulfur content. Based on the experimental findings, solution color has been changed from time to time due to spontaneous reaction. Researchers have described that faster deposition rate, larger sulfur and tin content could be seen for 5 minutes. SnS colloidal will be formed for 30 minutes, caused the tin and sulfur content will be reduced significantly. Optical properties indicated low transmission value (rough surface) and the band gap values were found in the range of 1 eV to 1.5 eV for the films prepared for 5 minutes. Heterojunction solar cell was designed with the zinc oxide (window layer) and CTSO (absorption layer). Photovoltaic effects (power conversion efficiency=0.049 %, fill factor=0.3, short circuit current=0.1 mA/cm^2, open circuit voltage=0.165 V) were studied according to the dark and illuminated I-V characteristics. It should be noted that poor crystallinity and low quality of cell structure caused very poor efficiency. Also, short diffusion length of carriers and formation of interface layer (ZnO and CTSO) hinders the electron flow caused very low short circuit current. at higher annealing temperature (850 °C to 1000 °C). The most intense peak was observed in (311) plane, and the crystallite size increased (27 nm to 32 nm) when the annealing temperature was incraesed. SEM images highlighted that different morphologies were found at 800 °C (spherical), 850 °C (spherical with high agglomeration) and 1000 °C (octahedral-like morphology). It was noticed that saturation magnetization increases when the temperature wasincreased based on the room temperature magnetic hysteresis (MH) loops (figure 5). The highest value was 28.2 emu/g at 1000 °C for 240 minutes. Because crystallinity increased, coercivity, magnetic anisotropy, crystal defects and internal strains were reduced. Finally, researcher pointed out that activation energy was 10.5 kJ/mol and crystallization of Ni- Zn ferrite films was followed first-order reaction (in randomnucleation). The Ni-Zn ferrite films have been used in telecommunication, microwaves devices, magnetic sensor, rod antennas, transformers cores and planar inductors. Because of several properties such as low coercivity, excellent magnetic properties and high resistivity. Several deposition techniques including dip coating, sputtering, pulsed laser deposition, chemical vapor deposition, and spray pyrolysis have been chosen for synthesize of thin films.However, these methods have disadvantages such as expensive equipment, restrictions on the selection of thesubstrate and high degree of control (equipment). $Ni_{0.5}Zn_{0.5}Fe_2O_4$ films were synthesized onto copper substrate [54] from electrolytic bath ($NiSO_4$, $(NH_4)_2Fe(SO_4)_2$ and $ZnSO_4$). In the XRD patterns, impurity (iron oxide) could beobserved at 800 °C, however single phase (spinel) appeared. Thin film based solar cells such as cadmium telluride (CdTe) and CuInGaSe have been used as an alternative to silicon based solar cells. However, cadmium was a toxic substance, while indium and gallium were considered rare elements (expensive materials). Cu2ZnSnS4 films could be used as absorbing material due to appropriate band gap (1.5 eV), higher absorption coefficients and less toxic elements. Previously, expensive deposition methods have been used to produce films. Production of p-type Cu2ZnSnS4 (CZTS) films onto flexible substrate (ITO substrates supported by polyethylene terephthalate) at room temperature [55], in nitrogen atmosphere (pH=5, deposition time=45 minutes, deposition potential=-1.05 V versus saturated calomel electrode) via electro deposition method. The photoelectrochemical properties of films were studied, and the prepared films indicated cathodic photocurrent. Single step growth of nanostructured films [56] onto ITO glass at room temperature (complexing agent=citric acid, pH=5, reference electrode=Ag/AgCl, counter electrode=platinum). In the transmittance measurements, it was noticed that 2.9%-3.4% and 2.2%-2.8% in the wavelength of 360nm to 560 nm, for as-deposited films and annealed films, respectively. Also, transmittance decreases rapidly in longer wavelength (560 nm to 620 nm) because ofhigher scattering of light and excellent crystallinity. In the x-ray diffraction (XRD) studies, it was noted that crystallite size increases in as-deposited films (7 nm to 45 nm), annealed films at 300 °C (22 nm to 31 nm) and annealed samples at 350 °C (24 nm to 72 nm) with increasing temperature. XRD patterns confirmed that the intensity of several peaks such as(112), (200), (105) and (204) planes increased when thetemperature was increased. From the SEM images, it was evidence that a variety of morphologies could be observed in as-deposited films (small grains with some sulfur clusters) and annealed samples (bigger flat grains with well-defined boundaries). Electrodeposition was performed using trisodium citrate as complexing agent and the deposition timewas 50 minutes [57]. In the XRD investigations, several diffractions peaks such as (112), (103) and (312) planes could be observed in annealed films. Crystallite size (12.27 nm to 37.22 nm) increases, but micro-strain (0.74×10^{-2} to 0.4×10^{-2}) and dislocation density (4.91x1016 to 0.72 x 1016 Lines/m2) decreased when the sulfurization temperature was increased from 350 °C to 425 °C based on the micro-structural data with (112) plane. In the Raman scattering measurements, there is single peak (at 336 cm^{-1}) could be seen, attributed to kesteritephase. Further, it was noted that no other ternary and binary compound could be observed in the Raman spectroscopy. Researchers have pointed out that a lower band gap was obtained with increasing temperature, indicating more energywas applied to improve crystallinity of the films. It was notedthat the films prepared at 425 °C (band gap=1.56 eV) showedthe best band gap value for solar cell applications if comparedto 350 °C (1.66 eV), 375 °C (1.64 eV), and 400 °C (1.6 eV). Deposition of films onto FTO glass [58] at deposition potential of -1.6 V and film thickness was about 1 μm. SEMimages showed the grain size was variable (a small part was less than 50 nm, and most are more than 100 nm).

Current potential properties of the films were studied when working electrode was immersed in $Fe(CN)^{4-}_{6}$ solution. Obviously, there was no change in photocurrent during the illumination process, because of conduction band mediated charge transfer mechanism. Experimental results revealed that almost no damage could be seen when the specific redox scavenger (sodium nitrite, formaldehyde, sodium sulfite) was used. Thegrowth of thin films has been described in conventional three- electrode cell [59] (reference electrode=saturated calomel electrode, temperature=room temperature, counter electrode=platinum, working electrode=molybdenum coated glass, pH=4.5 to 5, deposition time-45 minutes, deposition potential=-1.05 V, annealing atmosphere=argon, nitrogen, H_2S+N_2, deposition area=2 x 2 cm^2). The properties of these films were studied using XRD, FESEM, EDX, and UV-Visible spectrophotometer (Table 8). Solar cell (ITO/i-ZnO/CdS/CZTS) measurements with CZTS absorber prepared on molybdenum-coated soda lime glass substrate as reported by Shafaat. The highest power conversion efficiency was 7.3%, where the fill factor, open circuit voltage and short circuit current were found to be 58.1%, 567 mV, and 22 solar cell performance (open circuit voltage=540 mV, short circuit current=12.6 mA/cm^2, efficiency=3.16%) wasobtained in specific solar cells glass/Mo/CZTS/CdS/ZnO:Al/Al) with the zinc rich films. The p-type CuInGaSe (CIGS) films have been usedfor low-cost materials due to stability against photo- degradation, appropriate band gap value and excellent absorptivity value. The highest power conversion efficiency was obtained for the films prepared using co-evaporation method, however it seems very hard to scale up nowadays. One-step electrodeposition technique has been widely used to prepare thin films due to its advantages (simplicity, low-cost and scalability). Researchers found that the gallium and indium deposition efficiency was limited by H^+ reduction process in aqueous bath. Consequently, power conversion efficiency will be limited, and composition inhomogeneity surface will be observed. It is interesting to point out that electrodeposition of copper (E° = 0.342 V/NHE), indium (E° = −0.338 V/NHE), gallium (E° = mA/cm^2, respectively. Also, some leakage could be observed $In3+/In°$ $Ga3+/Ga°$ in the solar cell devices due to moderate shunt resistance (200 to 540 Ωcm^2). Quantum efficiency (QE) curve confirmed thata very weak response could be seen (wavelength is more than600 nm) due to high recombination losses in the bulk and depletion region. Araki and co-workers [60] have proposed that Cu-Zn-Sn precursors were sulfurized by annealing process (580 °C to 600 °C) in nitrogen atmosphere. The best −0.523 V/NHE), and selenium (E° = 0.74 V/NHE)was very challenging work due to they have different reduction potentials. Fei and co-workers [61] have reported the synthesis of films in alcohol solutions. It was noted that Ga^{3+} ions were very difficult deposition from other ions during the formation of CIGS films. This issue was solved byadding alcohol (LiCl dissolved in alcohol) in electrolytic bath. Alcohol gives wide electrochemical window, and the films were produced onto molybdenum foil (substrate) at deposition potential of -1.6 V versus SCE. Experimental findings indicated that annealed films (30 minutes, argon atmosphere, 550 □C) have uniform morphology (large grains=2 □m), good crystallization with the most intense peak at 2□=26.74□ (tetragonal phase) and copper poor composition. Rosalinda and co-workers [62] have demonstrated the production of films at the deposition potential of -1.15 V versus SCE (temperature=room temperature, substrates=molybdenum sheet, counter electrode=platinum mesh). It was noticed that evolution of hydrogen and formation of CIS films could be observed if the deposition potential was more than or less than -1.15 V. The obtained as-deposited films were characterized using XRD (amorphous phase), SEM (not uniform, cauliflower-like morphology), EDS (atomic percentage of copper, indium, gallium, and selenium was 16.8%, 8.9%, 3.7% and 70.5%) and band gap (1.7 eV) as reported. The growth of nanostructured films via electrodeposition method [63] in electrolytic cells (electrode is placed horizontal position). Properties of the films prepared using DC electrodeposition method and DC electro deposition plus mechanical perturbations are compared [Table 9]. Differences in atomic composition could be linked to the mass transport mechanism. It was noted that double layers will be producedin the surface of working electrode, and the mass transport by diffusion process when using DC electrodeposition. On the other hand, double layers have readjustment with each perturbation, and the mass transport by convection when employing DC electro deposition plus mechanical perturbations. A lower short circuit current (7.35 mA/cm^2) was observed due to irregular morphology, and leakage current happened and microcracks occurred. A lower fill factor (0.322) represents that the electrode must be improvedin future. RuiWei and co-workers [64] applied galvanometrymode to synthesis polycrystalline thin films onto molybdenum coated glass based on aqueous solutions of SeO_2, $CuCl_2$, $GaCl_3$ and $InCl_3$. During the formation of films, electro deposition was carried out by stirring (with magneticbar) to eliminate hydrogen generation. Researchers have highlighted that the properties of films could be controlled byvarying the deposition potential. SEM image revealed uniform morphology and compact surface could be seen at deposition potential of -1350 mV and -1550 mV versus SCE,respectively. However, rougher surface was obtained at higher potential (-1750 mV and -1950 mV). Surface roughness of the films prepared under different deposition times was studied using AFM. Roughness average (0.0483 to 0.2516□m), roughness root mean square (0.0606 to 0.296 μm), average height maximum (0.2354 to 0.7289 □m) and height maximum (0.4706 to 1.5879 μm) increase with increasing deposition time (20 seconds to 40 seconds at potential of -1350 mV). In terms of composition investigations, it was noted that gallium cannot be observed when the deposition potential was less than -1150 mV based on the EDX spectrum. The close stoichiometric films (Cu:In:Ga:Se=1:(1-x):x:2) could be seen when the deposition potential was -1550 mV. The CIGS films were synthesized through a two-electrode system [65], at deposition potential of -1.5 V, pH of 1.7. In the XRD studies, there are two peaks (2θ=35.34° and 42.11°) could be detected in the CIGS films with selenium dioxide if compared to pure selenium (2θ=35.34°). Because selenium dioxide was more soluble if compared to pure selenium, resulted in the crystallinity being increased. As shown in the SEM images, both samples showed irregular morphology, rough surface, and spherical shape. However, agglomeration on the surface of the substrate could be observed by using selenium dioxide. Solarcells were fabricated using ITO/CIGS/ZnS/ZnO device. Zincoxide and zinc sulfide acted as window layer and buffer layer, respectively. Higher efficiency was obtained in the films prepared using SeO_2 due to several reasons. These films have

smaller grain size, larger surface area and could store more energy. Also, these films have smaller crystal defects and greater band gap energy (can minimize the recombination). Other properties of CIGS prepared using pure selenium and selenium dioxide were highlighted in Table 10 [65]. Several diifraction peaks could be seen at (111), (200), (220)and (311) planes. Also, researchers have demonstrated that the movement of (111), (220) and (311) planes toward large angles, because of the replacement of selenium for sulfur. Finally, micro-strain (4.2 x 10^{-3}), crystallite size (34 nm) and dislocation density (0.00087 nm^{-2}) were reported as well. $AgInGaSe_2$ (AIGS) thin films have been used as tandem solar cells. The growth of AIGS films on molybdenum coated soda lime glass [66] and Corning glass substrates via molecular beam epitaxy (three-stage process). Composition studies revealed that the obtained films have small portion of $Ag(In,Ga)_5Se_8$ phase and tetragonal $Ag(In,Ga)Se_2$ phase. It was noted that more $Ag(In,Ga)Se_2$ phase could be observed with increasing the Ga/(In+Ga) atomic ratio. Researchers have described that the band gap of $Ag(In_{0.2}Ga_{0.8})Se_2$ films was 1.7 eV and these materials could be used as solar cell absorbers based on the photovoltaic properties (open circuit voltage=866 mV, short circuit current=14.5 mA/cm^2, efficiency=7.3%, fill factor=0.584). Zhang and co-workers [67] have pointed out that Ag-Se layerwas pre-deposited using lower temperature (350 □C), following that higher temperature (600 □C) was required for further process. The prepared Sg-Se layer can prevent the desorption of indium (high temperature process) from the films and could serve as cap layer. Based on the experimentalresults, the In/(In+Ga) ratio was 0.15 and the highest efficientreached 10.7%. The molecular beam epitaxy method has many disadvantages, even though this method has been used to prepare AIGS absorber materials successfully. Forinstance, it requires ultra-high vacuum atmosphere, high maintenance cost, and very complicated system. Xianfeng and co-workers [68] used non-vacuum technique to reduce the manufacturing cost and add sodium to improve the performance of the solar cells.

4. Penternary thin films

The $Cu_2NiSn(S,Se)_4$ film (CNTSSe) has been synthesized via electro deposition method, and followed by heat treatment process [69] in chalcogen vapor atmosphere. EDX spectrum highlighted that the composition of copper, nickel, tin, selenium, and sulphur was 20.2%, 11.6%, 12.47%, 22.72% and 33%, respectively, indicating close to stoichiometric films. SEM image shows homogeneous structure without cracks, big crystals, and thickness was 2.4 μm. Annealing of the precursors resulted in thicker films, because of the addition of selenium and sulfur in crystal lattice. EDX mapping (figure 6) indicated nickel rich, however tin, copper, and sulfur poor composition. It was noticed that selenium has been distributed uniformly over the surface of substrates. Based on the XRD data, tetragonal structure with polycrystalline was observed for the films produced onto glass/molybdenum substrates, subsequent heat treatment (30 minutes, 580 □C, in selenium & sulfur vapor). Synthesis of p-type $Cu_2ZnSnS_{4-x}O_x$ films (CZTSO) in a large area through electro deposition method (deposition area=1x1 cm^2, deposition time=20 minutes, pH=4.8, temperature=room temperature, reference electrode= SCE, electrolyte=$CuSO_4$, $ZnSO_4$, $SnSO_4$, $Na_2S_2O_3$, buffer solution=sodium lactate, working electrode= ITO glass) in a short time [70] under different deposition potential values. Film thickness, band gap, compositional of the prepared films were reported (Table 11). Auger electron spectroscopy (AES) was used to study the composition of the obtained samples. Obviously, a significant amount of oxygen (dissolved oxygen) could be observed in the films. Also, experimental results confirmed that the copper poor composition, but zinc and tin rich when the negative deposition potential was increased. Because of smaller ionization tendency in copper if compared to tin and zinc. Sample D showed the highest photocurrent based on the photo-electrochemical (PEC) measurements (figure 7), due to the smallest band gap value and less value of defect densities. Additionally, low optical transmission could be observed because of the scattering process. Rectification properties could be seen in the specifically designed heterojunction solar cells (CZTSO/ZnO/ITO). Lower power conversion efficiency due to high leakage current (0.15 mA/cm^2 at 1 V).

5. Conclusions

The electrodeposition method was used to prepare different types of thin films onto substrate. Generally, the three-electrode system consisted of counter, working and reference electrode. Experimental results confirmed that the properties of films depend on conditions such as pH, deposition time, annealing temperature, concentration of solutions, complexing agent, and deposition potential. XRD showed that amorphous phase and polycrystalline could be obtained in the as-deposited films and annealed samples. The obtained films could be employed in solar cell applications due to appropriate band gap value and large absorption coefficient.

Acknowledgements:

One of the authors (HO SM) would like to thank you to INTIInternational University, Malaysia for the financial support.

References

[1] N. Hasan, M. Sobuz, M. Khan and N. Mim. (2022). Integration of Rice Husk Ash as Supplementary Cementitious Material in the Production of Sustainable High-Strength Concrete. Materials. https:// doi.org/10.3390/ma15228171.

[2] L. Haitao, H. Zhou, S. Li and Z. Zheng. (2015). Fiber optic SERS microfluidic chip based on light induced gold nano-particle aggregation. Optics Communications. 352: 148-154.

[3] D. Hamed. (2021). Optical and electronic propertiesof lead sulfide spherical nano particle. Optik. https://doi.org/10.1016/j.ijleo.2021.166503

[4] J. Wang, J. Huang, W. Li and Z. Peng. (2023). Photovoltaic performance enhancement on

carbon counter electrode based PbS colloidal quantum dots solar cells with surface trap passivation via post- treatment process. Materials Science in semiconductor Processing. https://doi.org/10.1016/j.mssp.2023.107740.

[5] Y. Li, L. Xi, Z. Zhen and J. Liu. (2023). Mn-modified near surface atomic structure of CeO_2 nanorods for promoting catalytic oxidation of auto- exhaust carbon particles. Chemical Engineering Science. https://doi.org/10.1016/j.ces.2023.119309.

[6] N. Saravanan, K. Anuar, S.M. Ho and H. Abdul. (2010). Effect of deposition time on surface topography of chemical bath deposited PbSe thin films observed by atomic force microcopy. Pacific Journal of Science and Technology. 11: 399-403.

[7] C. Ayten, G. Hazal, T. Fulya and K. Hasan. (2023). Photovoltaic performance of magnetron sputtered antimony selenide thin film solar cells buffered by cadmium sulfide and cadmium sulfide/zinc sulfide. Thin Solid Films. https://doi.org/10.1016/j.tsf.2023.140070.

[8] S.M. Ho. (2017). Influence of deposition time on optical properties of chemically deposited nickel lead sulphide thin films. International journal of Applied Chemistry. 13: 111-120.

[9] A. Mario and A. Carlos. (2023). A direct correlationbetween structural and morphological defects of TiO_2 thin films on FTO substrates and photovoltaic performance of planar perovskite solar cells. Materials Science in semiconductor Processing. https://doi.org/10.1016/j.mssp.2023.107452.

[10] S.M. Ho. (2016). Synthesis and properties of cadmium oxide thin films: review. International Journal of Current Advanced Research. 5: 1038-1041.

[11] M. Patil, D. Lokhande, S. Khot and J. Patil. (2023). Nanocrystalline cobalt tungstate thin films prepared by SILAR method for electrocatalytic oxygen evolution reaction. International Journal of Hydrogen Energy. 48: 8465-8477.

[12] P. Mohammad, R. Sayed and G. Shahram. (2023). Nickel cobalt layered double hydroxide $NiCo_2S_4$/g-C_3N_4 nanohybrid for high performance asymmetric supercapacitor. International Journal of Hydrogen Energy. 48: 8127-8143.

[13] S. Yahia, V. Ganesh, S. Shek and D. Deivatamil. (2022). High responsivity n-ZnO/p-CuO heterojunction thin film synthesized by low-cost SILAR method for photodiode applications. Optical Materials. https://doi.org/10.1016/j.optmat.2022.112410.

[14] B. Moine, A. Pillonnet, J. Bulir and J. Lancok. (2017). In situ monitoring of electrical resistance during deposition of Ag and Al thin films by pulsed laser deposition: comparative study. Applied Surface Science. 418: 517-521.

[15] K. Ji, S. Lee and K. Kim. (2018). Photovoltaic property of n-ZnO/p-Si heterojunction grown by pulsed laser deposition. Thin Solid Films. 658: 22-26.

[16] X. Zhang, Q. Wei and T. Ken. (2019). Zinc morphology change in pulsating current deposition. Journal of Energy Storage. https://doi.org/10.1016/j.est.2019.100966.

[17] A. Souad. (2007). Characterization of electrodeposited Zn(Se,Te) thin films/polymer (PEO-chitosan blend) junction for solar cells applications. Universiti Malaya: Malaysia.

[18] P. Silvia, D. Viegas, A. Pasa and P. Cid. (2015). Electrochemical Cl doping of Cu_2O: structural and morphological properties. ECS Journal of Solid-State Science and Technology. 4: P181-P185.

[19] W. Xu, J. Song, Y. Lu and Z. Yu. (2011). Rapid fabrication of large area, corrosion resistant superhydrophobic Mg alloy surfaces, ACS Applied Materials & Interfaces. 3: 4404-4414.

[20] Z. Wang, Z. She and L. Li. (2012). Low-cost and large-scale fabrication method for an environmentally friendly superhydrophobic coating in magnesium alloy. Journal of Materials Chemistry. 22: 4097-4105.

[21] F. Su and K. Yao. (2014). facile fabrication of superhydrophobic surface with excellentmechanical abrasion and corrosion resistance oncopper substrate by a novel method. ACS Applied Materials & Interfaces. 6: 8762-8770.

[22] M. Dharmadasa and J. Haigh. (2006). Strengths and advantages of electro deposition as a semiconductor growth technique for applications in microelectronic devices. Journal of the Electrochemical Society. DOI 10.1149/1.2128120.

[23] D. Kim, H. Kim, J. Jeon and J. Oh. (2022). Annealing temperature effect on the surface properties and antimicrobial activity of SnSe thin films. Thin Solid Films. https://doi.org/10.1016/j.tsf.2022.139280.

[24] J. Singh and P. Rajaram. (2019). Single step electrode position of AlSb thin films. Materials Today: Proceedings. 16: 636-639.

[25] Y. Liu, Z. Zhu, Y. Cheng and B. Wei. (2021). Effectof electrodeposition temperature on the thin films ofZnO nanoparticles usedfor photocathodicprotection of SS304. Journal of Electro analytical Chemistry.

https://doi.org/10.1016/j.jelechem.2020.114945.

[26] O. Javier and C. Rubens. (2022). ZnOElectrodeposition Model for Morphology Control. Nanomaterials. https://doi.org/10.3390/nano12040720.

[27] O. Jun and T. Ohgai. (2021). Post-Annealing Effects on the Structure and Semiconductor Performance ofNanocrystalline ZnTe Thin Films Electrodeposited from an Aqueous Solution Containing Citric Acid. Applied Sciences. https://doi.org/10.3390/app112210632.

[28] Q. Adele and D. Teresa. (2013). Electro deposition of oriented cerium oxide films. International Journal of Electrochemistry. https://doi.org/10.1155/2013/482187.

[29] L. Li, C. Cheng and T. Teng. (2016). Electro deposition-based fabrication and characterization of tungsten trioxide thin film. Journal of Nanomaterials. https://doi.org/10.1155/2016/3623547.

[30] L. Shengjun, Y. Li, Z. Chen and W. Zhang. (2012).Electro deposition and low temperature post treatment of nanocrystalline SnO_2 films for flexible dye sensitized solar cells. Journal of Nanomaterials. https://doi.org/10.1155/2012/536810.

[31] A. El-Shaer and R. Abdelwahed. (2013). Potentiostatic Deposition and Characterization of Cuprous Oxide Thin Films. International Scholarly Research Notices. https://doi.org/10.1155/2013/271545.

[32] A. Maqsood, M. Jason, E. Robert and S. Thapa. (2014). Optimization of the electro deposition parameters to improve the stoichiometric of In_2S_3 films for solar applications using the Taguchi Method. Journal of Nanomaterials. https://doi.org/10.1155/2014/302159.

[33] H. Wenya, Z. Hanzhi, Z. Ye and L. Mengdi. (2015). Electro deposition and characterization of CuTe and Cu_2Te thin films. Journal of Nanomaterials. https://doi.org/10.1155/2015/240525.

[34] P. Celis, S. Nath and C. Srivastava. (2013). Simple formation of nanostructured molybdenum disulfide thin films by electrodeposition. International Journal of Electrochemistry. https://doi.org/10.1155/2013/138419.

[35] D. Lokhande and S. Pawar. (1987). Electrodeposition of $CuInTe_2$ films. Journal of Physics D: Applied Physics. DOI 10.1088/0022-3727/20/9/023..

[36] T. Ishizaki, A. Fuwa and N. Saito. (2004). Electro deposition of $CuInTe_2$ film from an acidic solution. Surface and Coatings Technology. 182: 156-160.

[37] L. Manorama and B. Nandu. (2014). Characterization of electrochemically deposited $CuInTe_2$ thin films for solar cell applications. Solar Energy Materials & Solar Cells. 123: 122-129.

[38] T. Mahalingam, S. Thanikaikarasan, C. Sanjeeviraja and K. Taekyu. (2010). Studies on Electroplated Copper Indium Telluride Thin Films. Journal ofNew Materials for Electrochemical Systems. 13: 77-82.

[39] C. Wang, S. Lu, J. Tang and Z. Li. (2018). Reactive close-spaced sublimation processed $CuSbSe_2$ thin films and their photovoltaic application. APL Materials. https://doi.org/10.1063/1.5028415.

[40] S. Rampino, M. Mazzer, M. Sidoli and S. Giulia. (2018). $CuSbSe_2$ thin film solar cells with ~4% conversion efficiency grown by low-temperature pulsed electron deposition. Solar Energy Materials and Solar Cells. 185: 86-96.

[41] Y. Bo, W. Chong, H. Song and Y. Zhao. (2017). Hydrazine solution processed $CuSbSe_2$: Temperature dependent phase and crystalorientation evolution. Solar Energy Materials and Solar Cells. 168: 112-118.

[42] T. Ding, Y. Jia, F. Liu and Y. Lai. (2011). One-step electrodeposition and annealing of $CuSbSe_2$ thin films. Electrochemical and Solid-state Letters.DOI 10.1149/2.007202esl.

[43] K. Abouabassi, L. Atourki, A. Sala and M. Ouafi. (2022). Annealing Effect on One Step Electrodeposited $CuSbSe_2$ Thin Films. Coatings. https://doi.org/10.3390/coatings12010075.

[44] S. Jiangshan, B. Li, Q. Zhang and Y. Rui, Y. (2021). Electrodeposited ternary $AgCuO_2$ nanocrystalline films as hole transport layers for inverted perovskite solar cells. Journal of Alloys and Compounds. https://doi.org/10.1016/j.jallcom.2021.161879.

[45] I. Armel, B. Amal, D. Soro and S. Mari. (2023). Growth of copper indium diselenide ternary thin films ($CuInSe_2$) for solar cells: Optimization of electrodeposition potential and pH parameters. Heliyon. DOI: 10.1016/j.heliyon.2023.e19057. Kaupmees, L., Altosaar, M., & Mellikov, E. (2007). Study of composition reproducibility of electrochemically co-deposited $CuInSe_2$ films onto ITO. Thin Solid Films. 515: 5891-5894.

[46] Y. Shen, W. Que, W. Huang and L. Cheng. (2010). Preparation and Characterization of $CuInSe_2$ Thin Films Derived by Electrodeposition Process for Solar Cells. Ferroelectrics. https://doi.org/10.1080/00150191003708802.

[47] K. Silva, W. Siripala, K. Blake and D. Jayanetti. (2001). Electrodeposition and characterization of

$CuInSe_2$ for applications in thin film solar cells. ThinSolid Films. 382: 158-163.

[48] A. Kashyout, E. Ahmed, T. Meaz and M. Amer. (2014). (One-step) electrochemical deposition and characterization of $CuInSe_2$ thin films. Alexandria Engineering Journal. 53: 731-736.

[49] H. Saidi, B. Durand and F. Boujmil. (2018). Elaboration and characterization of $CuInSe_2$ thin films using one step electrodeposition method on silicon substrate for photovoltaic application. Materials Research Express. https://doi.org/10.1088/2053-1591/aaa604.

[50] E. Shaker, S. Moataz and M. Kamal. (2012). Electrodeposited $CuInS_2$ using dodecybenzene sulphonic acid as a suspending agent for thin film solar cell. International Journal of Photoenergy. https://doi.org/10.1155/2012/918319.

[51] G. Rongfeng, G. Liu, Q. Sun and Y. Cao. (2015). Effects of preparation conditions on the $CuIns_2$ films prepared by one-step electro deposition method. Journal of Nanomaterials. https://doi.org/10.1155/2015/678929.

[52] N. Yuki and I. Masaya. (2012). Electrochemical Deposition of $Cu_xSn_ySz_O$ Thin Films and Their Application for Heterojunction Solar Cells. International Journal of Photoenergy. doi:10.1155/2012/171432.

[53] A. Saba, E. Elsayed, M. Rashad and M. Moharam.(2012). Electrochemical Synthesis of Nanocrystalline $Ni_{0.5}Zn_{0.5}Fe_2O_4$ Thin Film from Aqueous Sulfate Bath. ISRN Nanotechnology.doi:10.5402/2012/532168.

[54] M. Farinella, T. Spano, S. Piazza and C. Sunseri. (2014). Electrochemical deposition of CZTS thin films on flexible substrate. Energy Procedia. 44: 105–110.

[55] H. Rashid, J. Rabeya, M. Doha and O. Islam. (2018). Characterization of single step electrodeposited Cu_2ZnSnS_4 thin films. Journal of Optics. 47: 256-262.

[56] A. Ziti, F. Salah, L. Hicham and A. Batan. (2020). Growth and Characterization of CZTS Thin Films Synthetized by Electrodeposition Method for Photovoltaic Applications. IOP Conference Series: Materials Science and Engineering. doi:10.1088/1757-899X/948/1/012025.

[57] P. Sarswat, M. Free and G. Kumar. (2013). An investigation of nanocrystalline and electrochemically grown Cu_2ZnSnS_4 thin film using redox couples of different band offset. Journal of Spectroscopy. https://doi.org/10.1155/2013/321483.

[58] B. Pawar, M. Pawar, K. Gurav and Y. Lee. (2011). Effect of annealing atmosphere on the properties of electrochemically deposited Cu_2ZnSnS_4 (CZTS) thin films. International Scholarly research Notices. https://doi.org/10.5402/2011/934575.

[59] H. Araki, T. Akiko, Y, Makoto and W. Maw. (2009). Preparation of Cu_2ZnSnS_4 thin films by sulfurization of co-electroplated Cu-Zn-Sn precursors. Physica Status Solidi C: Current Topics in Solid State Physics. 6: 1266-1268.

[61] L. Fei, W. Wang, Z. Zou and J. Du. (2009). CIS(CIGS) thin films prepared for solar cells by one-step electrodeposition in alcohol solution. Journal of Physics: Conference Series. 152, doi:10.1088/1742-6596/152/1/012074.

[62] I. Rosalinda, C. Sunseri, R. Oliveri and S. Tiziana. (2013). Electrodeposition and Photo-electrochemical Behavior of CIGS Thin Films and Nanowire Arrays for Solar Cell. Chemical Engineering Transactions. 32: 343-348.

[63] B. Lara and M. Fernandez. (2019). Growth improved of CIGS thin films by applying mechanical perturbations to the working electrode during the electrodeposition process. Superlattices and Microstructures. 128: 144-150.

[64] Y. RuiWei, Y. Fu and K. Lew. (2014). Effect of Electrodeposition Potential on Composition of $CuIn_{1-x}Ga_xSe_2$ Absorber Layer for Solar Cell by One-Step Electrodeposition. International Journal of Photoenergy. http://dx.doi.org/10.1155/2014/478428.

[65] R. Hilda, N. Mufti, Z. Siti and H. Abadi. (2022). Electrodeposition Technique to Fabrication CIGS using Pure Selenium and SeO_2 as Selenium Source. Malaysian Journal of Fundamental and Applied Sciences. 18: 367-373.

[66] K. Yamada, N. Tokio and N. Hoshino. (2006). Crystallographic and electrical properties of wide gap $Ag(In_{1-x},Ga_x)Se_2$ thin films and solar cells. Science and Technology of Advanced Materials. 7: 42-45.

[67] X. Zhang, K. Tsuyoshi and Y. Akira. (2013). Deposition of $Ag(In,Ga)Se_2$ Solar Cells by a Modified Three-Stage Method Using a Low-Temperature-Deposited Ag–Se Cap Layer. Japanese Journal of Applied Physics. DOI 10.7567/JJAP.52.055801. Xianfeng, Z., Sun, Q., Wang, Y., & Duan, Z. (2020). Solar Cell Applications of Solution-Processed $AgInGaSe_2$ Thin Films and Improved Properties by Sodium Doping. Nanomaterials. doi:10.3390/nano10030547.

[68] A. Stanchik, T. Asmalouskaya, V. Rakitin and V. Gremenok. (2022). Morphology and Crystal Structure of $Cu_2NiSn(S,Se)_4$ Thin Films Obtained by an Electrodeposition-Annealing

Process. Coatings. https://doi.org/10.3390/coatings12081198.

[69] Y. Kai and I. Masaya. (2012). Fabrication of Cu–Zn–Sn–S–O Thin Films by the Electrochemical Deposition Method and Application to Heterojunction Cells. International Journal of Photoenergy. doi:10.1155/2012/154704.